Review of Recent Activities on the Tagged Neutron Method at FLNP JINR

Yuri Kopatch

for the TANGRA collaboration

ISINN-31, Dongguan China, May 26-30, 2025

The Tagged Neutron Method or Associated Particle Technique

H. H. BARSCHALL, I . ROSEN, R. F. TASCHEK, J. H. WILLIAMS, Rev. Mod. Phys., V. 24, 1 (**1952**): Since neutrons arise only from nuclear reactions, there always exist at the time of their formation one or more charged particles associated with each neutron. In some cases a one-to-one correspondence exists between neutron and charged particle, and the counting of these charged particles with known efficiency determines the associated neutron flux.

$$D+D \rightarrow He^{3}+n+Q$$
$$D+T \rightarrow He^{4}+n+Q$$

J.D.L.H. Wood, A SEALED-OFF 14 MeV NEUTRON SOURCE INCORPORATING A SOLID STATE ALPHA-PARTICLE DETECTOR, Nucl. Instr. Meth., pp.49-52, Jan.-Feb. **1963**.

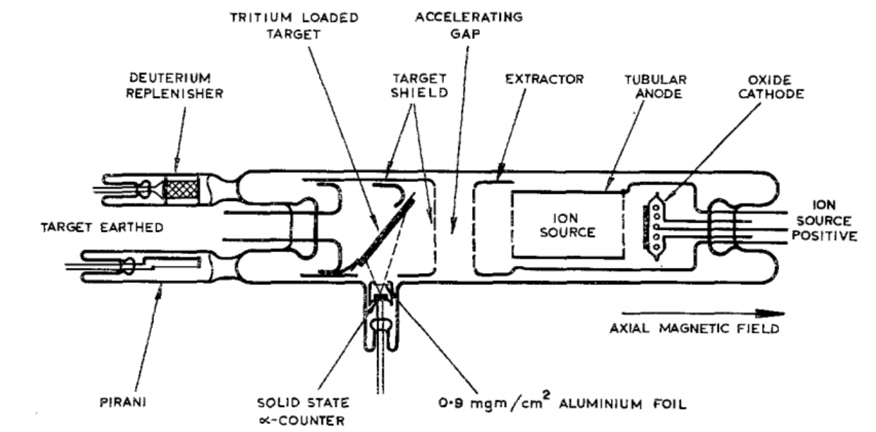

Development and Applications of the Tagged Neutron Method at JINR

At the end of 1990th **V.M.Bystritsky** and **M.G.Sapozhnikov** proposed to study the tagged neutron method using the Van de Graaff EG-5 electrostatic accelerator at FLNP. The first experiments were started in 1999.

The first installation had a tritium target of 1.7 curie, a single-channel alpha detector based on ZnS and a gamma detector made of a NaI(Tl) crystal with a diameter of 200 mm.

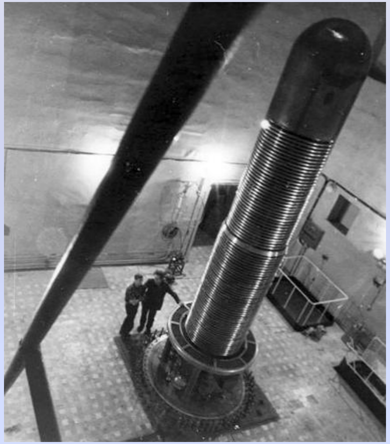

~5 m

An important stage in the development of the TNM was the creation of a portable neutron generator, which was carried out by the N.L. Dukhov All-Russian Research Institute of Automatics, Moscow (**VNIIA**) in 2003, according to the technical specifications developed at JINR.

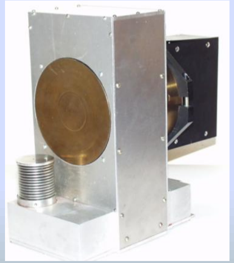

~30 cm

Portable VNIIA ING-27 n-generators



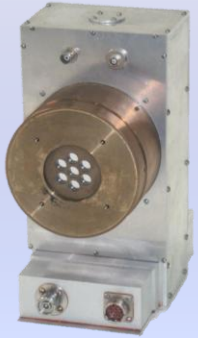




Neutron generators

Some characteristics of commercial neutron generators

Type of NG	Metherial of α-detecor	Number of tagged beams	Pixel size (mm)	Distance between pixels (mm)
Sodern, Euritrack	Si	64	5.8	0.2
API-120	YAP	256	3	-
ING-27	Si	9	10	1
ING-27-64	Si	64	6	1
ING-27-256	AsGa	256	4	0,1

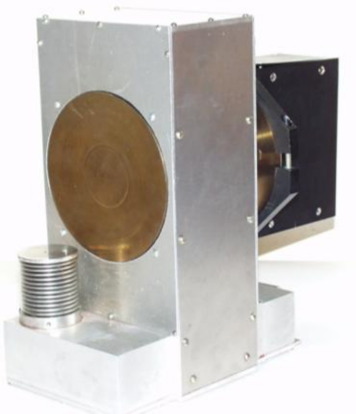

Produced by

N.L. Dukhov All-Russian Automation Research Institute

Main characteristics:

Maximal intensity	~$5 \cdot 10^{7}$ c^{-1}
Neutron energy	14.1 МэВ
Neutron radiation mode	steady-state
Operation time	~800 hours

The Tagged Neutron Method with ING-27 compact neutron generators

$D + T \rightarrow {}^{4}He\ (3.5MeV) + n\ (14.1MeV)$

The 14.1 MeV neutron is tagged in time and direction by detecting the associated α-particle released in the opposite direction.

Main advantages of the method:

- **significantly reduced background**
- **direct measurement of the neutron flux**
- **position sensitivity**
- **possibility to select time-correlated events using coincidences**

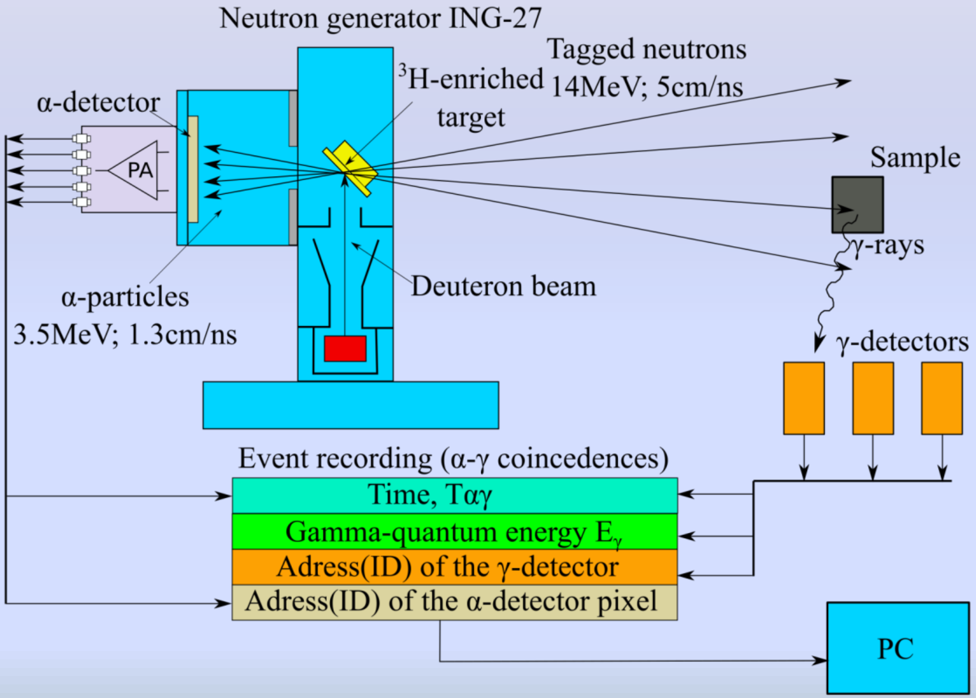

Application of the TNM: detection of hazardous substances

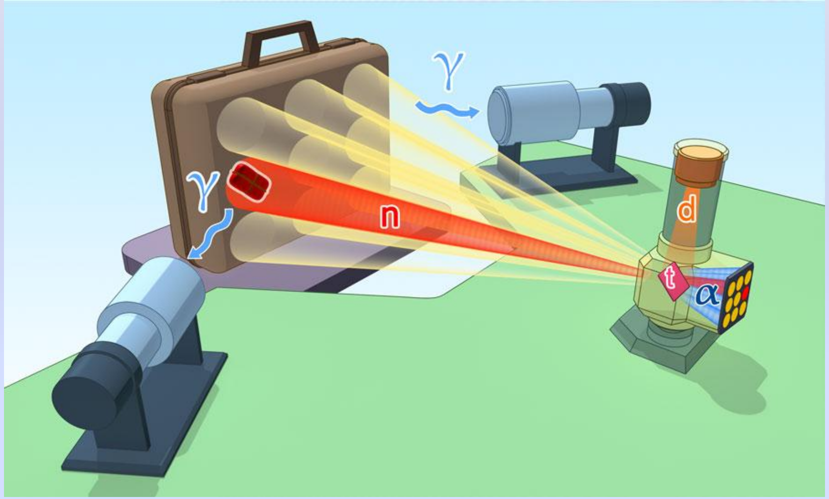

DVIN-1 is a portable system designed for detecting concealed explosives in inspected objects.
The **DVIN-1** analyzes the elemental composition of substances and can identify over **30 explosive materials.** The key advantage of **DVIN-1** over gas analyzers is its ability not only to detect the possible presence of explosives but also to **pinpoint their exact location** within the inspected object.

Application of the TNM: elemental composition of minerals

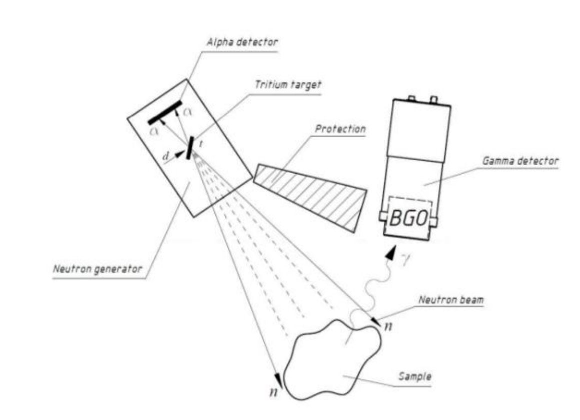

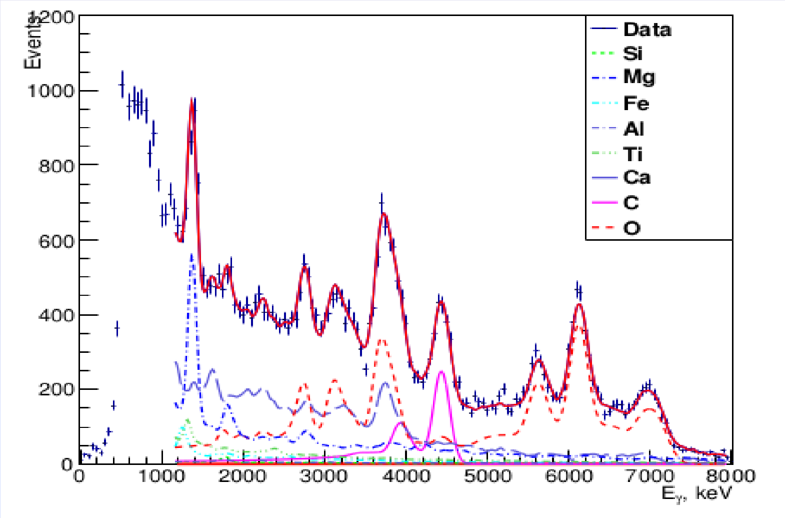

Decomposition of the spectrum from dolomite ($CaCO_3xMgCO_3$)

Mass fraction of oxides according to chemical analysis and as a result of fit procedure.

	SiO_2	MgO	FeO	Al_2O_3	CaO	CO_2
SE2843	47.16	6.66	11.69	15.67	10.97	0.44
SE2843 TNM	48.5 ± 4.4	8.2 ± 1.3	15.2 ± 2.3	13.8 ± 3.3	12.3 ± 4.0	2.0 ± 2.4
SE2869	2.29	0.68	0.	0.	53.35	42.3
SE2869 TNM	0.4 ± 1.4	0.3 ± 0.6	0.00 ± 0.6	4.8 ± 1.8	47.4 ± 2.8	47.2 ± 2.5

V.Yu. Alexakhin et al, reported at ISINN-23, Dubna (2015)
V.Yu. Alexakhin et al, preprint of JINR (2015)

Application of the TNM: Search for large diamonds in kimberlite ore

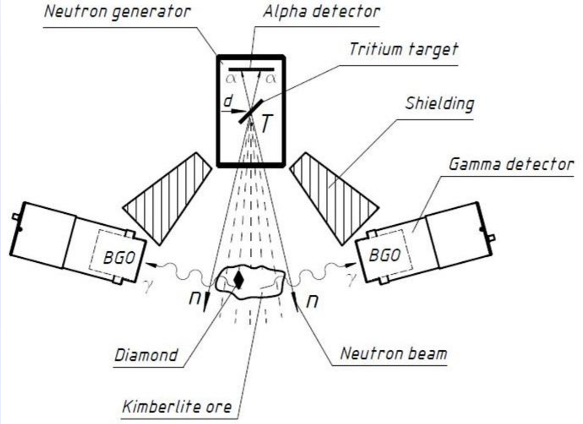

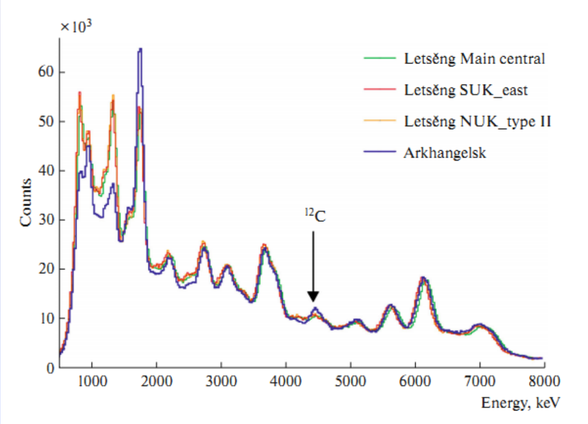

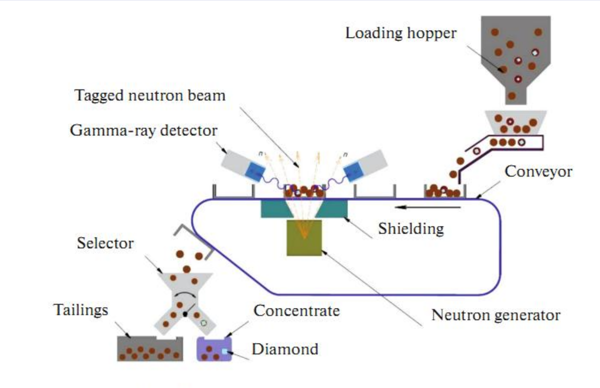

Fig. 24. General schematic view of the pilot separator.

- Kimberlite ore is irradiated by 14.1 neutrons from the neutron generator.
- Characteristic γ-ray spectra are measured by the BGO detectors and analyzed separately for each ING-27 voxel.
- The condition for finding the diamond is a local excess of the count rate for gamma-rays with energies ~4.43 MeV (characteristic line of carbon)

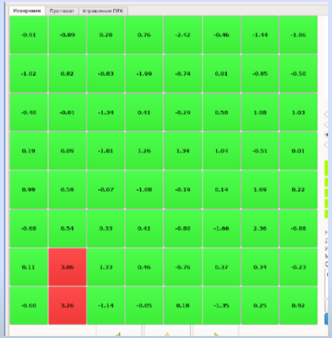

-0.91	-0.89	0.28	0.76	-2.42	-0.46	-1.44	-1.86
-1.02	0.82	-0.83	-1.99	-0.74	0.01	-0.85	-0.50
-0.40	-0.01	-1.34	0.41	-0.29	0.58	1.08	1.03
0.19	0.09	-1.81	1.26	1.34	1.04	-0.51	0.01
0.99	0.59	-0.07	-1.08	-0.19	0.14	1.69	0.22
-0.68	0.54	0.33	0.41	-0.80	-1.66	2.36	-0.88
0.11	3.86	1.33	0.46	-0.76	0.37	0.34	-0.23
-0.60	3.26	-1.14	-0.05	0.18	-1.35	0.25	0.92

Design of an ore separator

- Separator productivity 1060 kg/h.
- Minimum diamond size 8 mm.
- False detection probability 3%.

Yu.N. Rogov et al, reported at ISINN-24, Dubna (2016)

Project TANGRA @ JINR: TAgged Neutrons and Gamma RAys

Development of the tagged neutron method for determining the elemental structure of matter and nuclear reactions research

Main participants:

- ***JINR (FLNP, VBLHEP, DLNP, LRB), Dubna, Russia***
- ***N.L. Dukhov All-Russian Automation Research Institute, Moscow, Russia.***
- ***Lomonosov Moscow State University, Moscow, Russia.***
- ***INRNE, Bulgarian Academy of Sciences, Sofia, Bulgaria***
- ***Institute Ruđer Bošković, Zagreb, Croatia***
- ***BHU Varanasi, India***
- ***LLC DIAMANT, Dubna, Russia***

Multi-detector gamma-ray spectrometry system “Romashka”

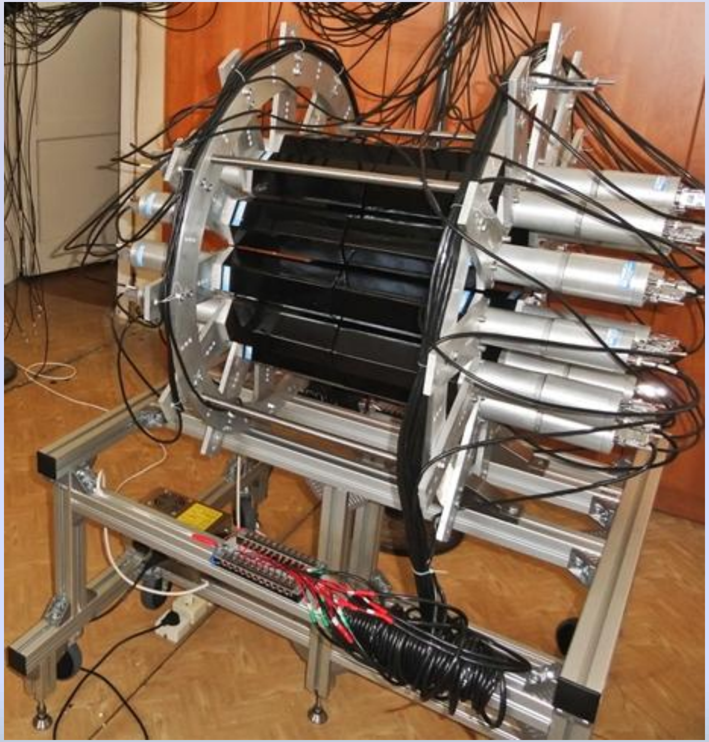

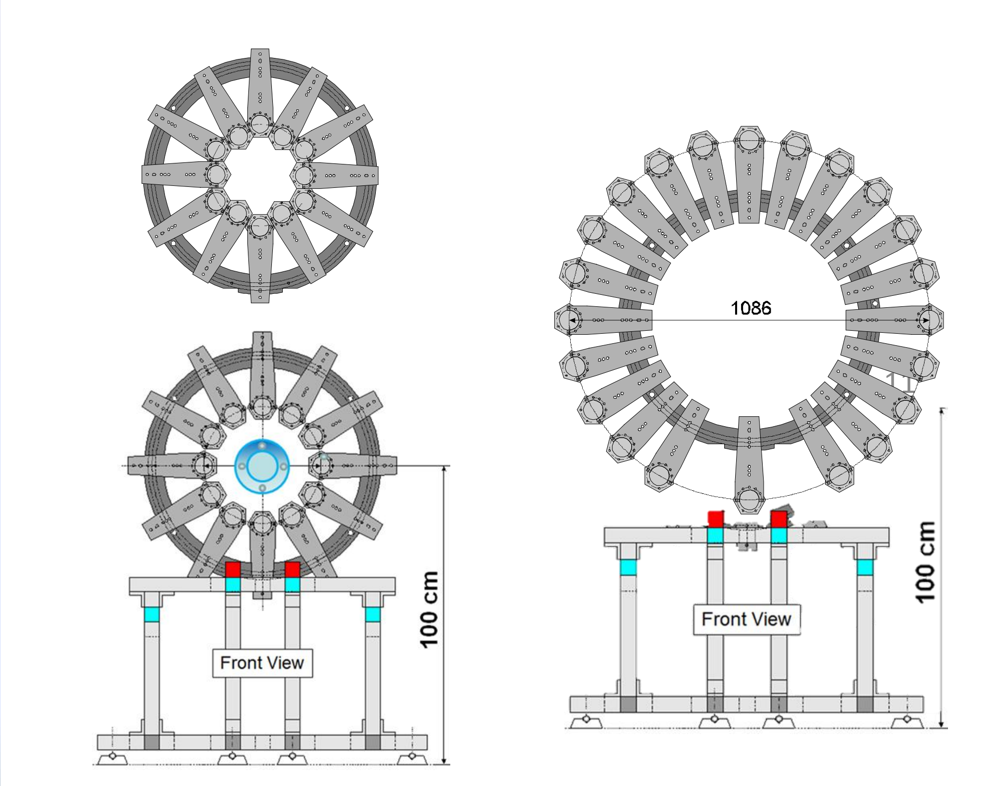

Using gamma-ray detector system "Romashka" with TNM

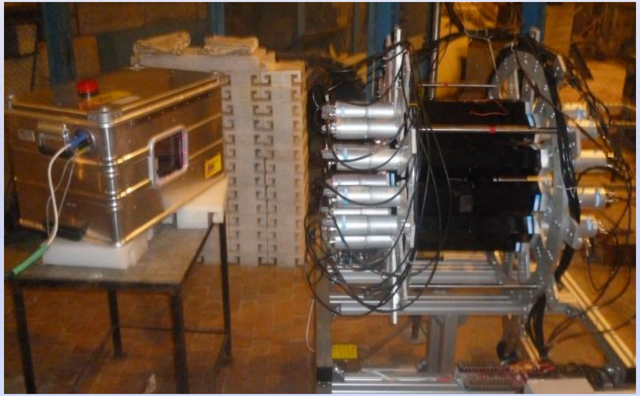

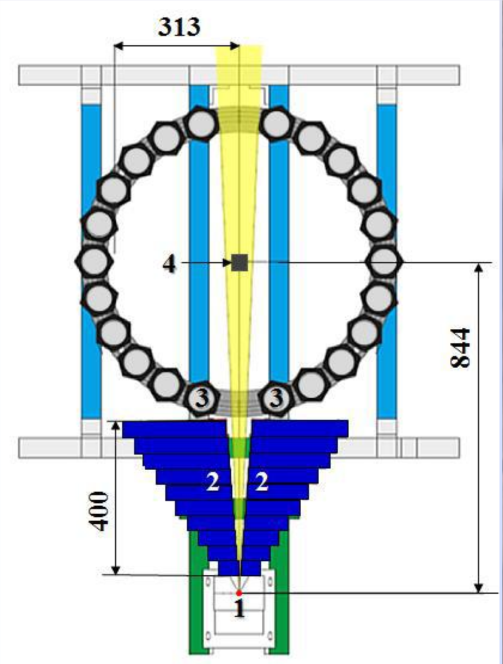

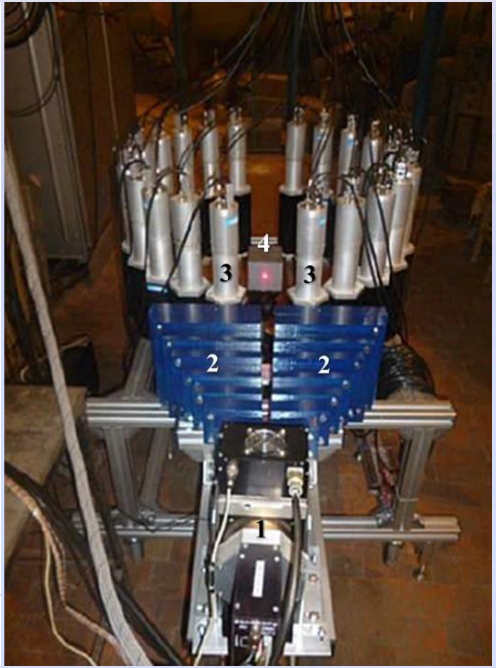

Various configurations of gamma-ray detectors

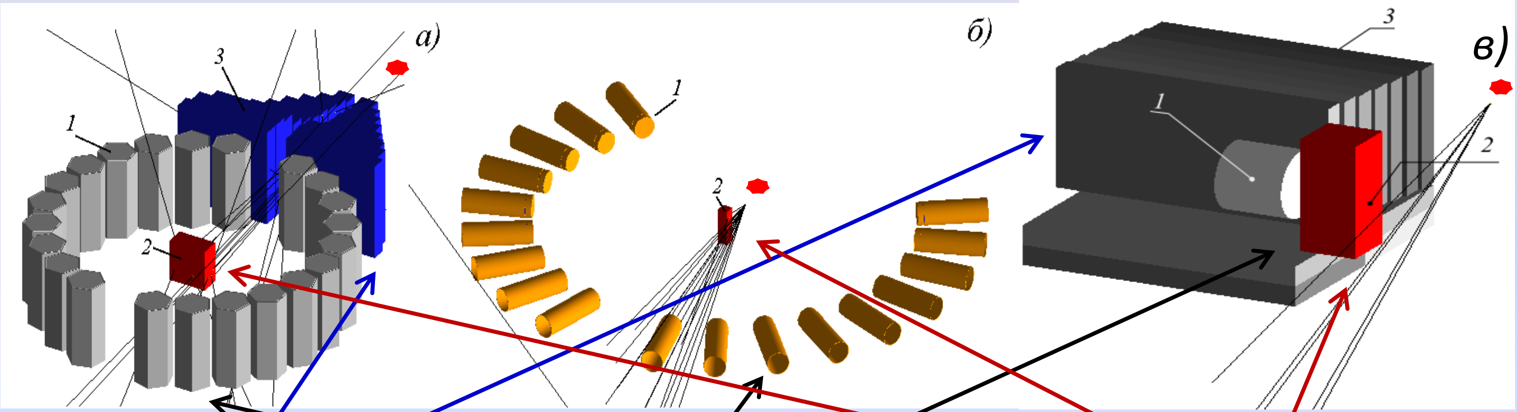

Shielding **Detectors** **Sample**

22 NaI(Tl) detectors **18 BGO detectors** **1 HPGe detector**

Angular distributions of γ-rays from inelastic scattering of 14.1 MeV neutrons

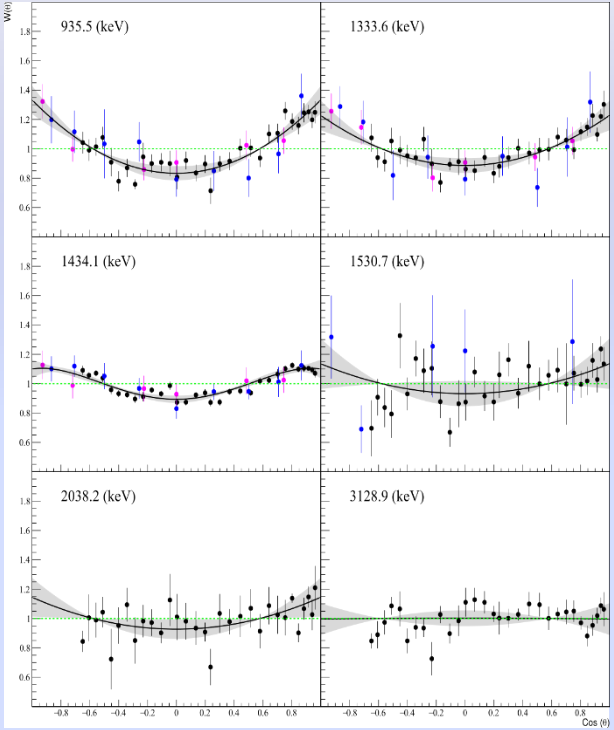

Angular distributions of γ-rays for chromium

Angular distributions of γ-rays are the normalized differential cross sections:

$$\frac{d\sigma}{d\Omega}(\Theta) = \frac{\sigma^{\gamma}}{4\pi} W(\theta) \qquad W(\theta) = 1 + \sum_{I=2,4\ldots}^{2J} a_I P_I(\cos\theta)$$

Eγ (keV)	Ref.	a_2	a_4
935.5	**Our work**	**0.34 ± 0.02**	*
	Abbodanno1973	0.35 ± 0.09	*
	Oblozinsky1992	0.27 ± 0.06	*
1333.6	**Our work**	**0.23 ± 0.02**	*
	Abbodanno1973	0.41 ± 0.09	*
	Oblozinsky1992	0.30 ± 0.05	*
1434.1	**Our work**	**0.16 ± 0.01**	**-0.06 ± 0.02**
	Abbodanno1973	0.18 ± 0.05	-0.06 ± 0.07
	Oblozinsky1992	0.13 ± 0.03	0.03± 0.04
1530.7	Oblozinsky1992	-0.12 ± 0.31	*
	Our work	**0.14 ± 0.05**	*
2038.2	**Our work**	**0.15 ± 0.04**	*
3128.9	**Our work**	**0.01 ± 0.03**	

Table of gamma-ray yields for chromium

E_γ (keV)	Reaction	J_i^P (E_i, keV)	J_j^P (E_j, keV)	Y_γ, %		
				Our work	[42]	[3]
124,4	^{52}Cr(n,p)^{52}V	(141,6)	(17,2)	2,4 (0,5)		
226,3	^{50}Cr(n,p)^{50}V	(226,2)	(0)	3,0 (0,6)		
320,1	^{52}Cr(n,d)^{51}V	(320,1)	(0)	2,2 (0,8)		1,8 (0,1)
567,0	^{52}Cr(n,n')^{52}Cr	(4039,2)	(3472,2)	5,0 (0,9)		
600,2	^{52}Cr(n,n')^{52}Cr	(4015,5)	(3415,3)	10,0 (1,6)		
645,7* 647,5*	^{52}Cr(n,p)^{52}V ^{52}Cr(n,n')^{52}Cr	(793,5) (3415,3)	(147,8) (2767,8)	8,5 (1,0)		 8,9 (0,3)
704,5	^{52}Cr(n,n')^{52}Cr	(3472,2)	(2767,8)	-		5,4 (0,2)
744,2* 749,1*	^{52}Cr(n,n')^{52}Cr ^{52}Cr(n,2n)^{51}Cr	(3113,9) (749,1)	(2369,6) (0)	12,3 (1,5)	16,3 (2,9)	9,1 (0,3) 5,4 (0,2)
783,3	^{50}Cr(n,n')^{50}Cr	(783,3)	(0)	4,2 (0,5)		
791,3	^{52}Cr(n,2n)^{51}Cr	(4563,0)	(3771,7)	2,9 (0,5)		
834,9	^{54}Cr(n,n')^{54}Cr	(834,9)	(0)	3,1 (0,4)		
848,2	^{52}Cr(n,n')^{52}Cr	(3615,9)	(2767,8)	7,3 (0,5)		
935,5	**^{52}Cr(n,n')^{52}Cr**	**(2369,6)**	**(1434,1)**	**33,5 (0,8)**	**26,9 (3,8)**	**30,3 (1,2)**
1164,6	^{52}Cr(n,2n)^{51}Cr	(1164,6)	(0)	-		4,6 (0,2)
1246,3* 1247,7*	^{52}Cr(n,n')^{52}Cr	(3615,9) (4015,5)	(2369,6) (2767,8)	5,8 (0,9)		5,0 (0,2)
1289,5	^{53}Cr(n,n')^{53}Cr	(1289,5)	(0)	3,3 (0,7)		
1333,7	**^{52}Cr(n,n')^{52}Cr**	**(2767,8)**	**(1434,1)**	**26,4 (0,8)**	**22,1 (4,0)**	**26,2 (1,0)**
1434,1	**^{52}Cr(n,n')^{52}Cr**	**(1434,1)**	**(0)**	**100**	**100**	**100**
1530,7	**^{52}Cr(n,n')^{52}Cr**	**(2964,8)**	**(1434,1)**	**6,8 (0,6)**	**9,5 (3,0)**	**5,1 (0,2)**
1727,7* 1730,4*	^{52}Cr(n,n')^{52}Cr	(3161,7) (4100,0)	(1434,1) (2369,6)	5,7 (0,7)		3,3 (0,1)
2038,2	**^{52}Cr(n,n')^{52}Cr**	**(3472,2)**	**(1434,1)**	**1,7 (0,5)**		
2257,7	^{52}Cr(n,n')^{52}Cr	(4627,3)	(2369,6)	1,1 (0,5)		
2337,6	^{52}Cr(n,n')^{52}Cr	(3771,7)	(1434,1)	2,1 (0,6)		
3128,9	**^{52}Cr(n,n')^{52}Cr**	**(4563,0)**	**(1434,1)**	**2,0 (0,7)**		

TNM with high resolution gamma spectrometry

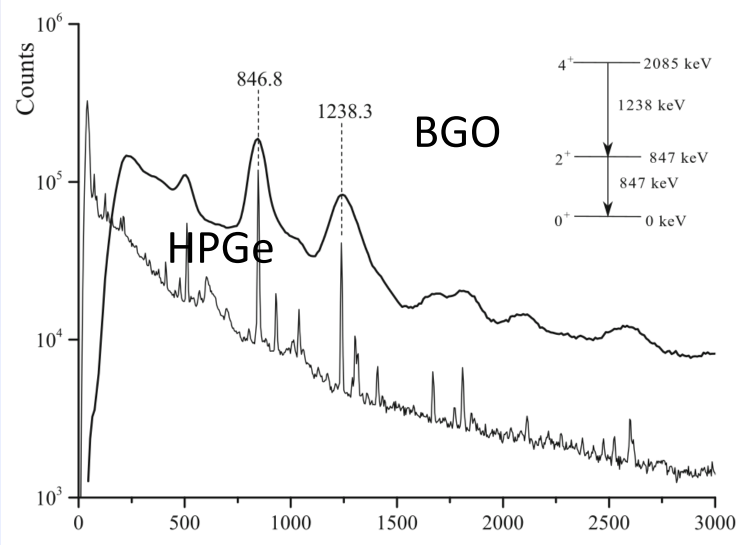

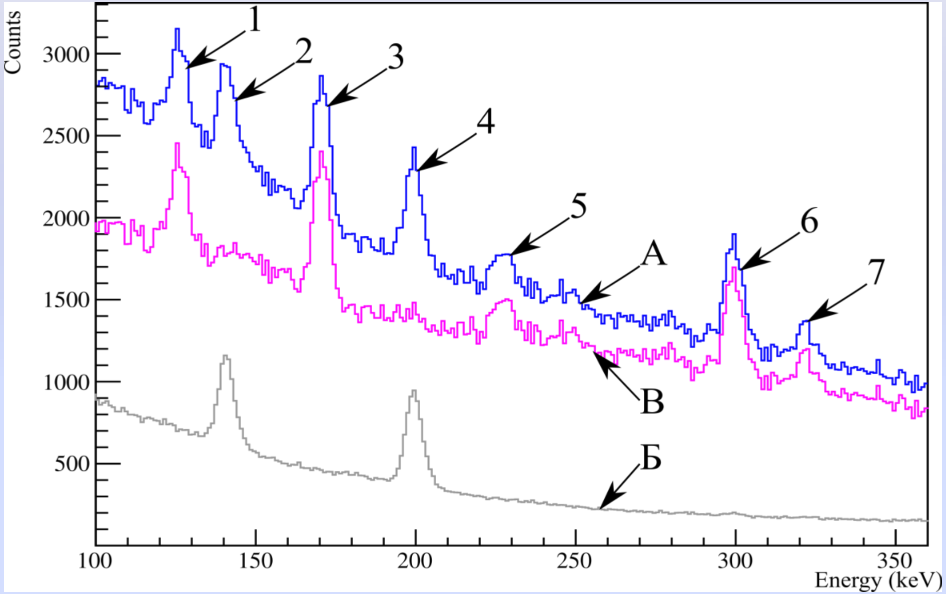

– energy spectrum in the coincidence window

– random background in the same coincidence window

– Pure spectrum after background subraction

Developing and optimizing signal processing techniques for the TANGRA project experimental setups

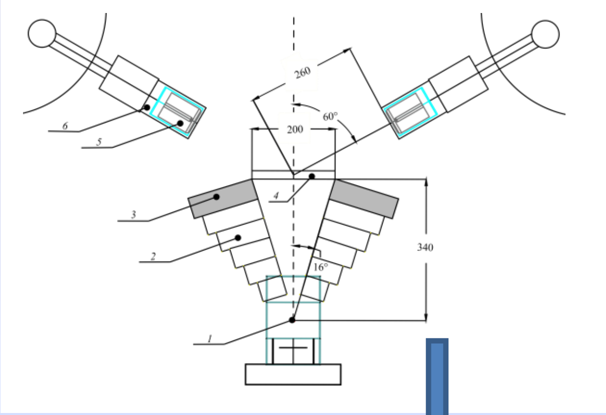

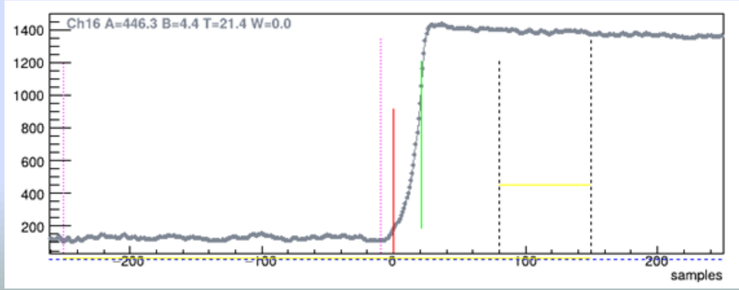

How?

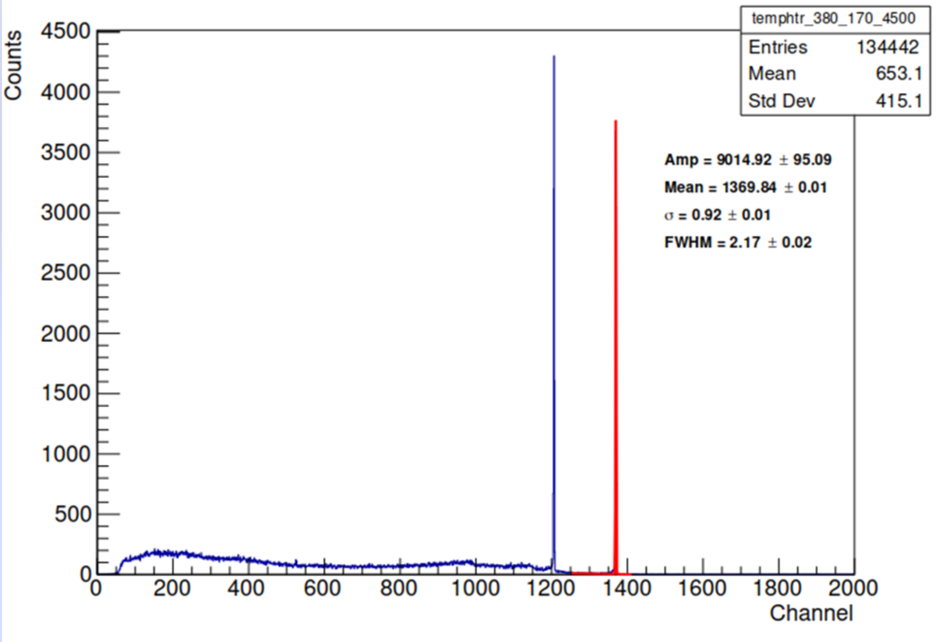

See report of P. Kharlamov at ISINN-31

New experimental setup

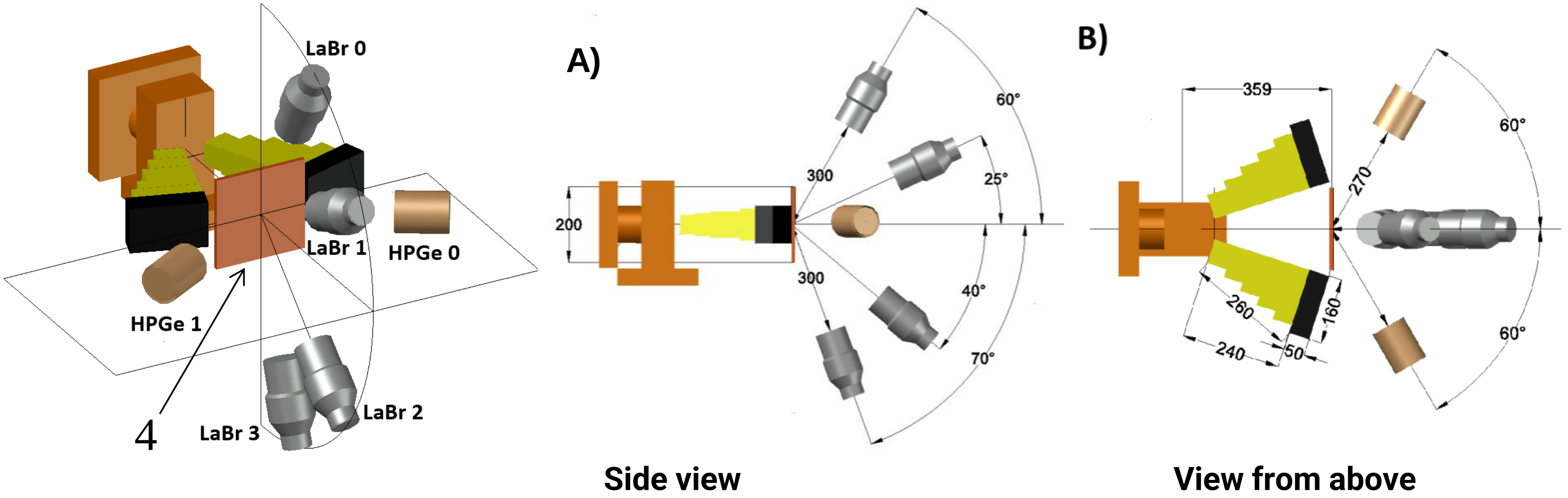

Setup for measurement of differential cross sections of γ-ray emission. Includes 2 HPGe and 4 $LaBr_3$ detectors. The geometry is optimized using Geant4.

See report of D. Grozdanov at ISINN-31

Data analysis:

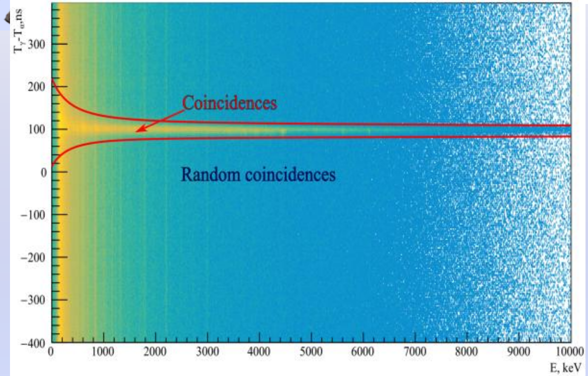

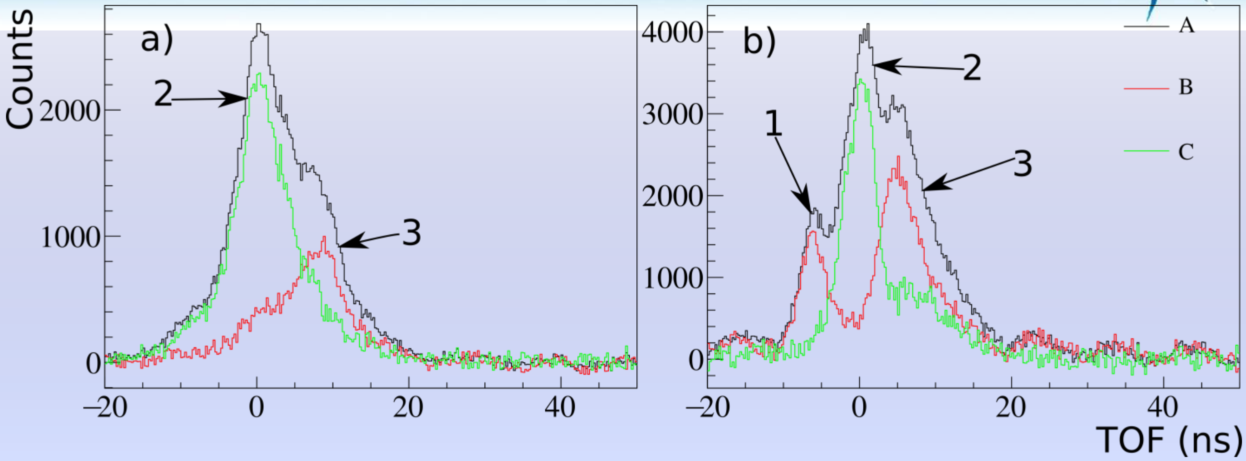

Diagram energy (E_γ) – the time between the registration of a γ–quantum and its corresponding α-particle (T_γ - T_α) formed as a result of reactions in the sample, with a highlighted coincidence window.

Example of time spectra (in the energy window of about 1 – 2 MeV) for HPGe detector a) and LaBr detector b).

Where: A – With sample, B – Without sample, C – Difference.
1 – is γ-from (Fe – Pb) - Collimator, 2 – γ from sample, 3 – is scattered neutrons

See report of D. Grozdanov at ISINN-31

Differential cross sections of gamma-ray emission: current and expected results

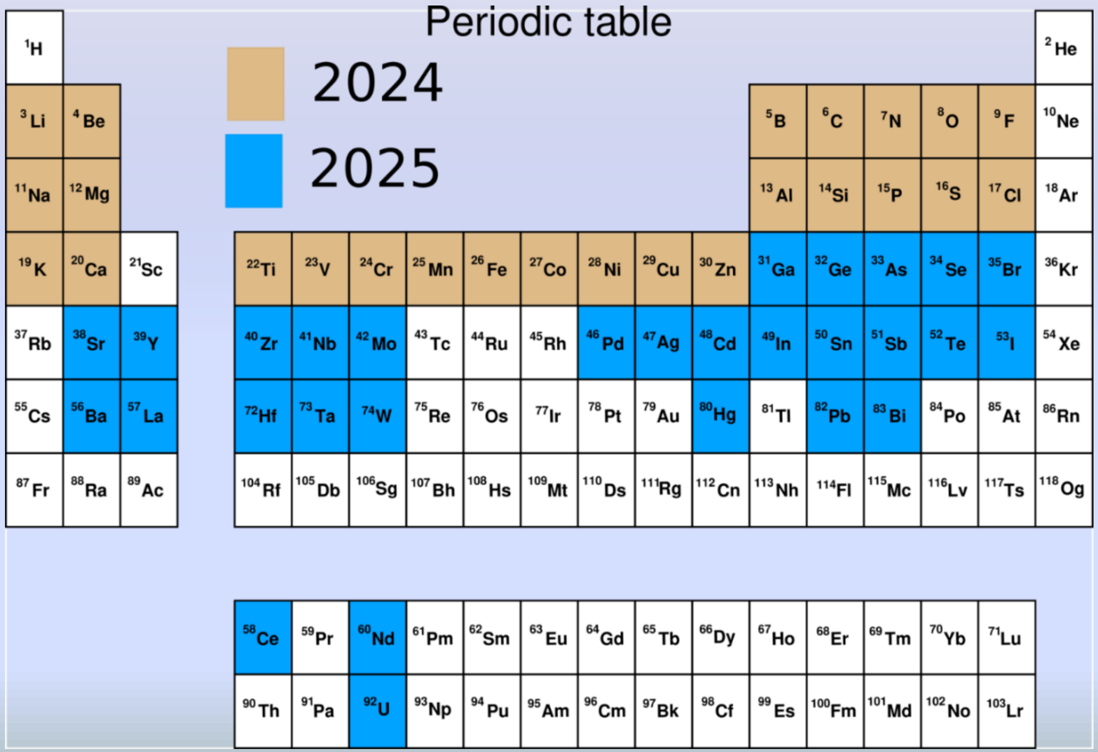

Determination of the efficiency of the detector sysmem. Analysis of chlorine neutron capture experiment for efficiency calculation validation

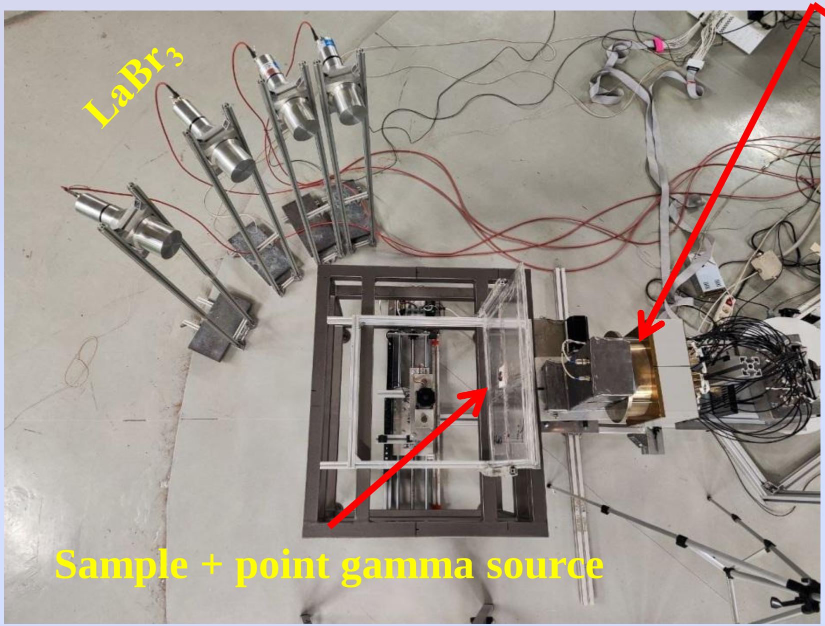

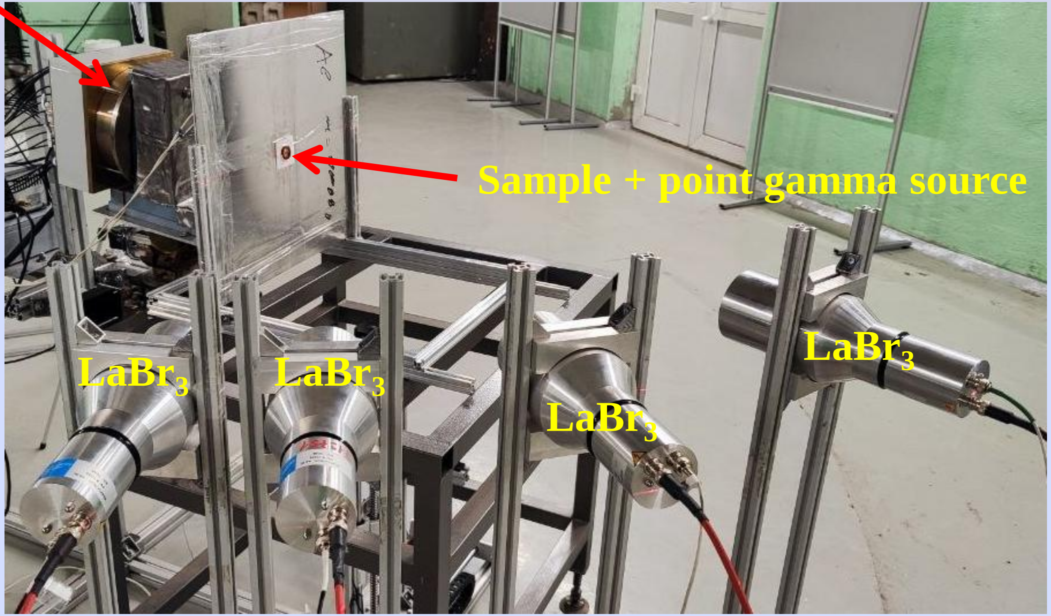

See report of C. Hramco at ISINN-31

Measurement of differential cross sections of neutron scattering on 12C

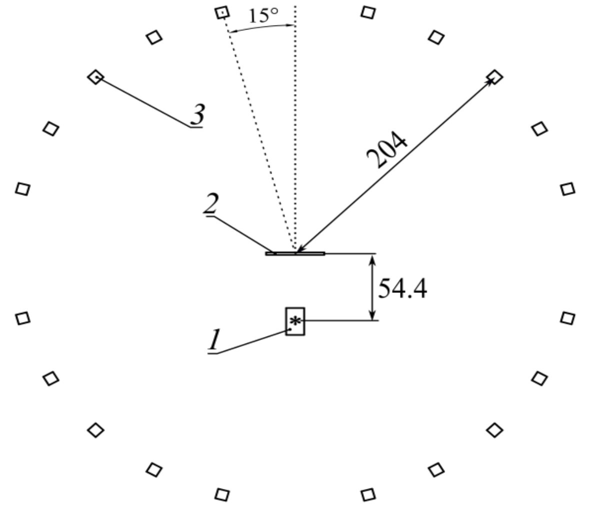

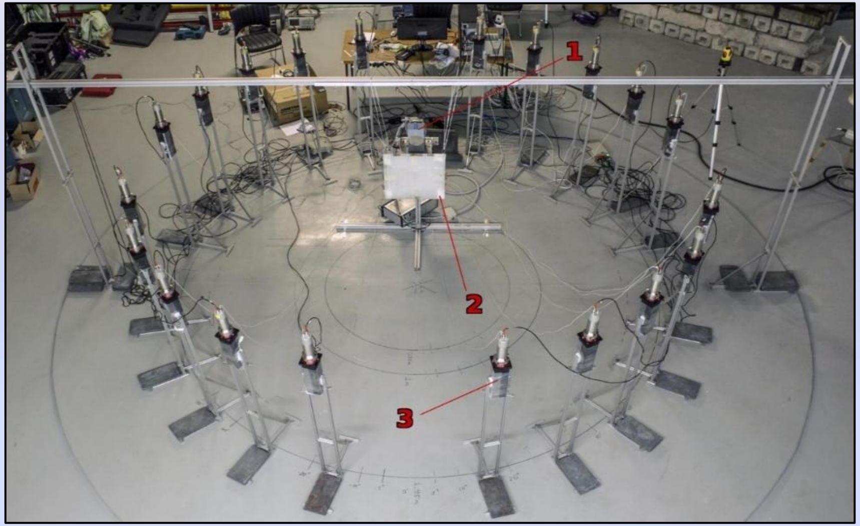

Scheme of the experimental setup with plastic detectors for measuring angular distributions of the scattered neutrons. *1* – ING-27 neutron generator, *2* – irradiated carbon sample, *3* – one of the 20 plastic detectors used in the registration system.

Neutron source: ING-27 generator

Sample: graphite block, 44 cm x 44 cm x 2 cm

Neutron detectors: polyphenyltoluene scintillators

Measurement of differential cross sections of neutron scattering on 12C

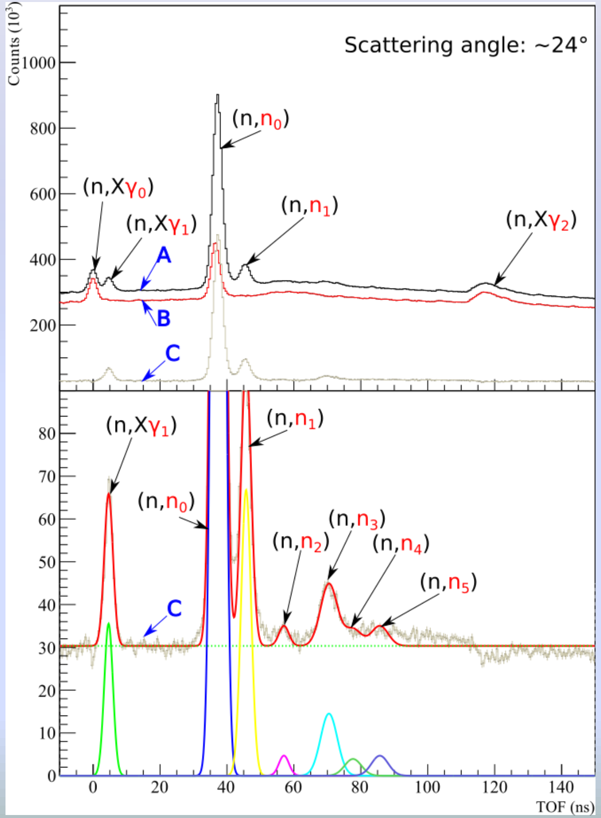

Examples of the time-of-flight spectra obtained. Peaks are labelled with source reaction, registered particle is painted red.

A – is measurement with target (^{12}C), Time ~ 48h;

B – is measurement without target (Background), Time ~ 28h,

C – Net spectra (without background)

$(n,X\gamma_0)$ – γ from ING-27

$(n,X\gamma_1)$ – γ from target (^{12}C)

$(n,X\gamma_2)$ – γ from the opposite wall

(n,n_0) - elastic scattering

(n,n_1) - inelastic scattering to the 1 excited state of ^{12}C 4.44MeV

(n,n_2) - inelastic scattering to the 2 excited state of ^{12}C 7.65MeV

(n,n_3) - inelastic scattering to the 3 excited state of ^{12}C 9.64MeV

(n,n_4) - inelastic scattering to the 4 excited state of ^{12}C 10.30MeV

(n,n_5) - inelastic scattering to the 5 excited state of ^{12}C 10.84MeV

Characterization of an EJ-200 plastic scintillator array for experiments with 14-MeV tagged neutrons

The experimental setup consisting of 20 plastic EJ-200 scintillators

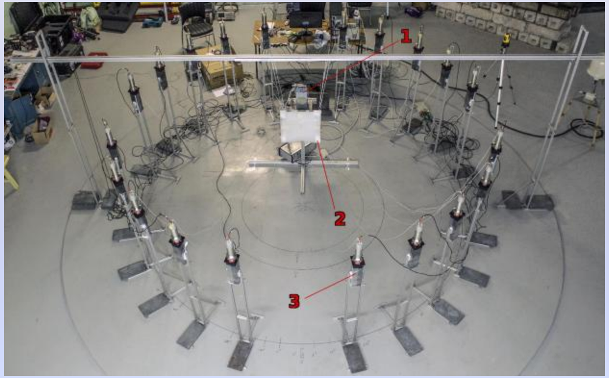

The measured light output function for protons in comparison with other datasets

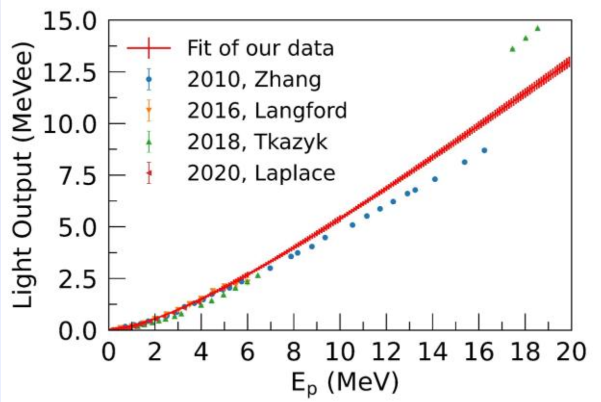

The measured efficiency values vs the GEANT4 simulation

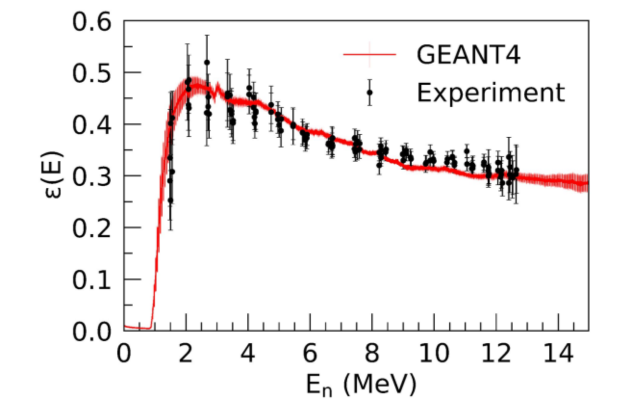

- The new approach based on the tagged neutron method has been implemented to characterization of the organic scintillator based detectors. It was based on scattering of neutrons on carbon and hydrogen nuclei.
- The light output functions for protons and α-particles were measured
- The detection efficiency was experimentally measured relative to the the standard of the cross section of the elastic scattering of neutrons on hydrogen
- The results obtained has been used to calculate the cross section in the experiments on investigation of the neutron emission

See report of P. Prusachenko at ISINN-31

Experimental and theoretical study of (n-n′-γ) angular correlations

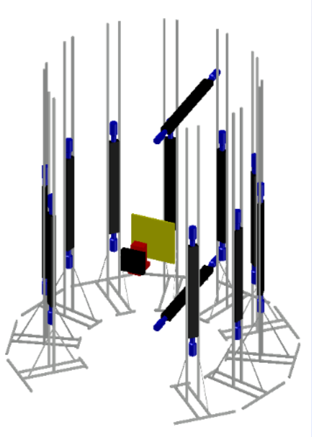

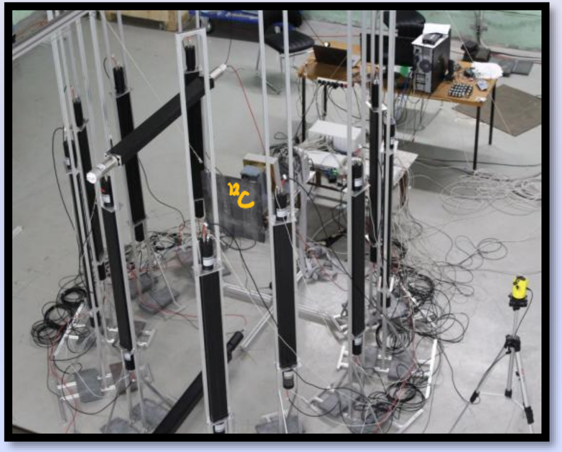

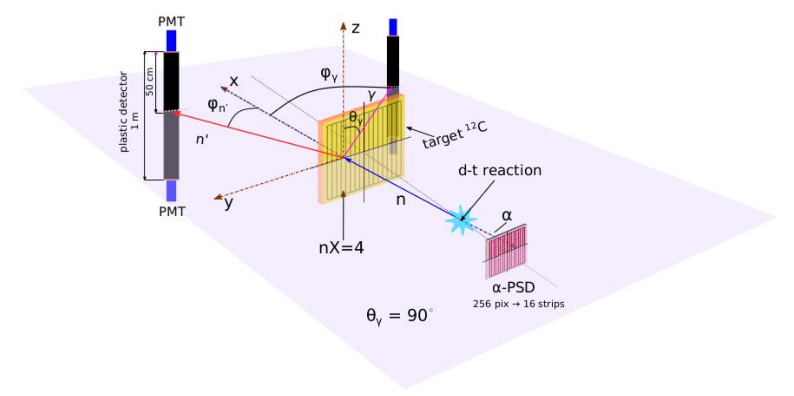

- 10 long (1 m) plastic scintillator detectors with 2 PMT made by EPIC CRYSTALL
- Detectors are placed at angles from 15° to 135° with step 30°
- 2 long detectors are placed above and below the target

(n′,γ) correlations are important for:

- **Understanding the reaction mechanism**
- **Testing the theoretical predictions**
- **Checking for nuclear forces invariance for *n* and *p***

See report of P. Filonchik at ISINN-31

Investigation of triple (n-n′-γ) correlations: theoretical description

Differential probability of gamma-quanta emission dependence on inelastic scattered neutron direction

$$dw(\vec{n}_\beta,\vec{n}_\gamma) = A \sum_{Q=0,2,4,\dots}\sum_{\Lambda\Lambda'} D^{\Lambda}_{\Lambda' Q}\,\phi^{\Lambda}_{\Lambda' Q}(\vec{n}_k,\vec{n}_\beta,\vec{n}_\gamma)\,d\Omega_\beta d\Omega_\gamma$$

$$A = \frac{\omega\, a_L(e)^2}{2\hbar c^3 k_\alpha k_\beta r_\beta^2}\,\frac{m_\beta}{m_\alpha},$$

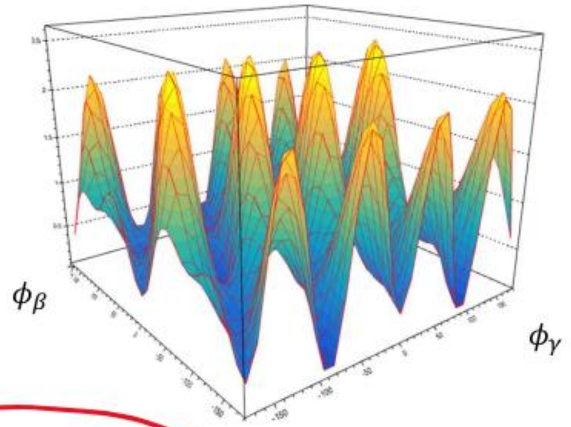

$$D^{\Lambda}_{\Lambda' Q} = \sqrt{2Q+1}\,C^{L1}_{L1Q0}\,U(I_f I_i L Q, L I_i)\sqrt{(2I_i+1)(2\Lambda'+1)}\ \times$$

$$\sum_{JJ'} g_{J'} \sum_{l_\alpha l'_\alpha j_\alpha j'_\alpha l_\beta l'_\beta j_\beta j'_\beta} S_J(l_\alpha j_\alpha \to l_\beta j_\beta)\, S^*_{J'}(l'_\alpha j'_\alpha \to l'_\beta j'_\beta)\sqrt{(2J+1)(2j'_\beta+1)}\ \times$$

$$C^{l_\alpha 0}_{l'_\alpha 0 \Lambda 0} C^{l_\beta 0}_{l'_\beta 0 \Lambda' 0}\, U(s j'_\alpha l_\alpha \Lambda, l'_\alpha j_\alpha)\, U(I_\alpha J' j_\alpha \Lambda, j'_\alpha J)\, U(s j'_\beta l_\beta \Lambda', l'_\beta j_\beta) \begin{Bmatrix} J & j_\beta & I_i \\ J' & j'_\beta & I_i \\ \Lambda & \Lambda' & Q \end{Bmatrix}.$$

S-matrix coefficients from TALYS

See report of P. Filonchik at ISINN-31

THEORETICAL DESCRIPTION OF ANGULAR DISTRIBUTION OF GAMMA RADIATION OF NEUTRON-NUCLEAR REACTION PRODUCTS

TABLE 1. Parameters of the optical potential

Model of excitation	Symmetric rotational optical model				Model of excitation	Symmetric rotational optical model		
^{12}C	V_v	W_v	R_v	a_v	^{28}Si	V_v	R_v	a_v
	54.7	0.47	1.098	0.48		50.77	1.15	0.61
	W_D		R_D	a_D		W_D	R_D	a_D
	1.94		1.26	0.42		6.59	1.15	0.58
	W_{SO}		R_{SO}	a_{SO}		V_{SO}	R_{SO}	a_{SO}
	6.51		0.85	0.67		6.0	1.15	0.58

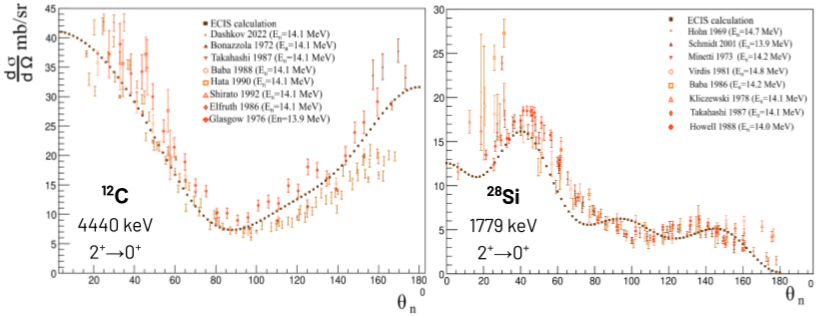

FIG 1. Differential cross section of inelastic scattering of a neutron by ^{12}C and ^{28}Si

TABLE 2. Parameters of angular distributions of γ quanta

	Authors	Legendre polynomials coefficients			Authors	Legendre polynomials coefficients	
		α_2	α_4			α_2	α_4
^{12}C 4440 keV $2^+\to0^+$	Bystritsky 2016	0, 34 (0.02)	-0, 33 (0.02)	^{28}Si 1779 keV $2^+\to0^+$	Abbondanno 1973	0.16 (0.06)	—
	Benveniste 1960	0.37 (0.05)	-0.39 (0.07)		Hong-Yu Zhou 2010	0.21 (0.02)	—
	Tangra 2018	0.42(0.02)	-0.27 (0.02)		Tangra 2018	0.20 (0.03)	—
	Theoretical calculation	0.33	-0.39		Theoretical calculation	0.28	-0.33

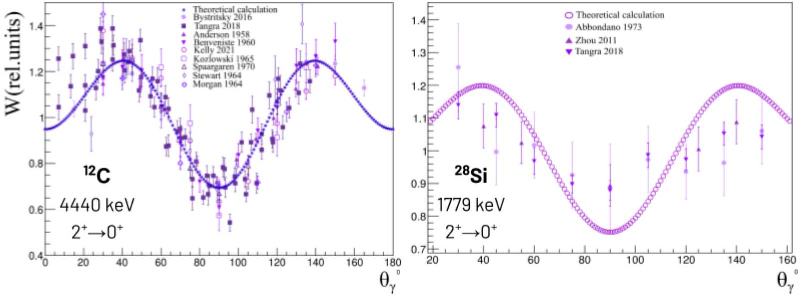

FIG 2. Angular distribution of γ radiation for ^{12}C and ^{28}Si

See poster of A. Andreev at ISINN-31

Determination of carbon concentration in soil using the tagged neutron method

BGO detectors

distribution of reactions by depth

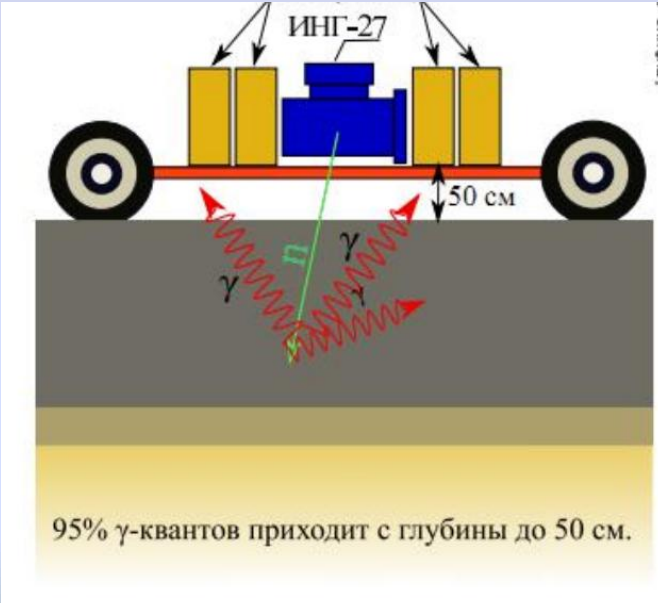

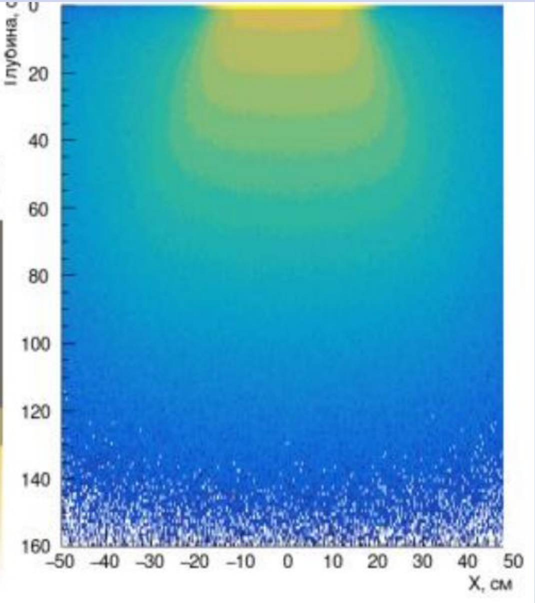

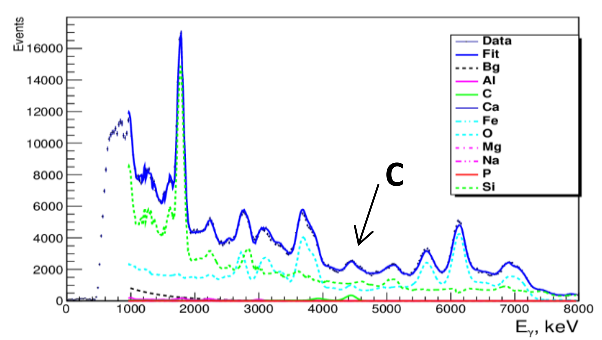

Carbon concentration is determined by the amplitude of the characteristic 4.44 MeV gamma-line.

NAS: Neutron Analyzer of Soil

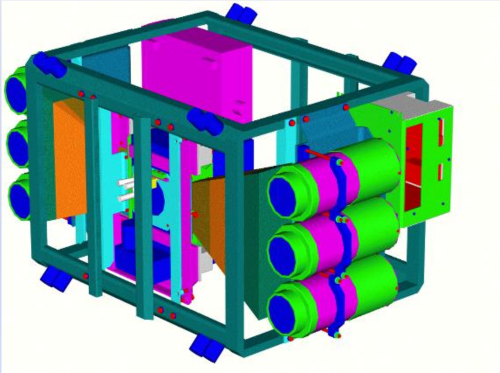

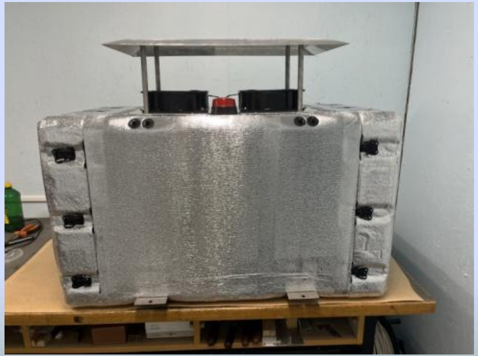

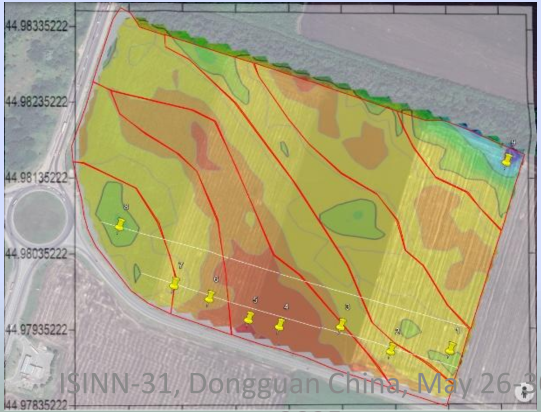

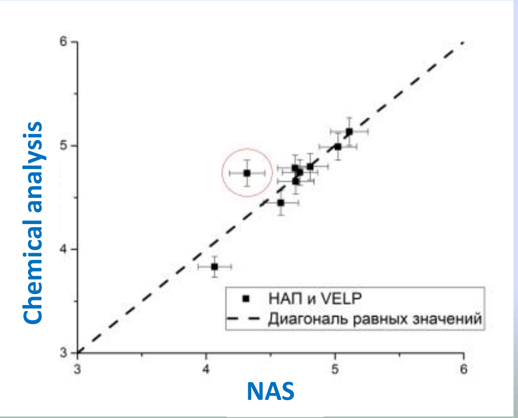

Conclusions

The tagged neutron method (TNM) is an effective tool for studying the reactions of fast neutrons with nuclei, which makes it possible to successfully implement a program for measuring differential cross sections of neutron scattering and γ-ray production, as well as a program for the application of the TNM for non-destructive elemental analysis.

Acknowledgements:

Grozdanov D.N, Prusachenko P.S., Fedorov N.A., Tretyakova T.Yu., Pampushik G.V., Andreev A.V., Skoy V.R., Hramco C., Filonchik P.G., Kharlamov P.I., Barabanov A.L., Ruskov I.N., Sapozhnikov M.G., Rogov Yu.N., Alexakhin A.Yu., Razinkov E.A., Borisov D.N., Negovelov S.I.

Supported by the RSCF grant 23-12-00239

Thank you for your attention!